

Published in final edited form as:

*Opt Lett.* 2012 April 1; 37(7): 1193–1195.

## Time-gated Cerenkov emission spectroscopy from linear accelerator irradiation of tissue phantoms

Adam K. Glaser<sup>1</sup>, Rongxiao Zhang<sup>3</sup>, Scott C. Davis<sup>1</sup>, David J. Gladstone<sup>2</sup>, and Brian W. Pogue<sup>1,2,3</sup>

<sup>1</sup>Thayer School of Engineering, Dartmouth College, Hanover, NH 03755

<sup>2</sup>Norris Cotton Cancer Center, Dartmouth-Hitchcock Medical Center, Lebanon, NH 03766

<sup>3</sup>Department of Physics and Astronomy, Dartmouth College, Hanover, NH 03755

### Abstract

Radiation from a linear accelerator induces Cerenkov emission in tissue, which has recently been shown to produce biochemical spectral signatures which can be interpreted to estimate tissue hemoglobin and oxygen saturation or molecular fluorescence from reporters. The Cerenkov optical light levels are in the range of  $10^{-6}$ – $10^{-9}$  W/cm<sup>2</sup>, which limits the practical utility of the signal in routine radiation therapy monitoring. However due to the fact that the radiation is pulsed, gated-acquisition of the signal allows detection in the presence of ambient lighting, as is demonstrated here. This observation has the potential to significantly increase the value of Cerenkov emission spectroscopy during radiation therapy to monitor tissue molecular events.

Optical photon emission is observed when a charged particle moves faster than the speed of light in a given dielectric medium<sup>1</sup>. This phenomenon, known as Cerenkov emission, has found applications in the field of optical molecular imaging through Cerenkov luminescence imaging (CLI), a novel technique for tracking  $\beta$ -emitting radionuclides *in vivo*<sup>2–6</sup>. Additionally, linear accelerator (LINAC) induced Cerenkov emission spectroscopy (CES) has recently been investigated for both fluorescence and absorption spectroscopy methods<sup>7,8</sup>. As a result of the exponential dependence of Cerenkov photon yield with particle energy, the optical emission per particle from a 6–24 MeV LINAC beam is approximately 2–3 orders of magnitude greater than Cerenkov emission from isotopic  $\beta$ -emitters which are typically less than 1 MeV. As such, the CES signal strength during external beam radiotherapy (EBRT) is reasonably high ( $10^{-6}$ – $10^{-9}$  W/cm<sup>2</sup>) and could potentially be used for clinical disease treatment and monitoring. While sufficiently high to measure, it is still well below room light levels, which is a challenge for practical use. In this study, we address the issue of signal acquisition during ambient room lighting, by demonstrating gated detection of Cerenkov emission from a LINAC when operating in standard pulsed delivery mode.

Previous CES studies have relied on continuous wave (CW) signal collection in the absence of ambient lighting<sup>7,8</sup>. While commercial incandescent lights have an irradiance of  $10^{-1}$  to  $10^{-3}$  W/cm<sup>2</sup>, the Cerenkov emission irradiances from a LINAC or PET agent are roughly  $10^{-6}$  –  $10^{-9}$  W/cm<sup>2</sup> and  $10^{-8}$  –  $10^{-12}$  W/cm<sup>2</sup>, depending directly upon the dose rate of irradiation. These large differences in optical irradiance make CW detection of Cerenkov emission impossible in the presence of ambient light. PET agent CES works through

imaging in a closed environment with a near complete absence of light. In comparison though, LINAC radiation is produced in pulsed microseconds-long bursts, as generated by the accelerator waveguide. Thus, by taking advantage of a linear accelerator's inherent pulsed operation, time-gated detection of Cerenkov emission is possible to significantly improve the signal to ambient light ratio.

The linear accelerator (Varian LINAC 2100C, Varian Medical Systems, Palo Alto, CA) used in this study delivers a 5  $\mu$ s radiation pulse every 5 ms, resulting in a potential  $\sim 1000\times$  rejection of room light during gated detection. As a result, under dimmed room lighting conditions the ambient and Cerenkov optical signals are nearly equivalent in intensity. Additionally by picking up light directionally from the tissue using fiber optics or a lens system, it is feasible to increase the Cerenkov signal over the ambient room light by at least 1–2 orders of magnitude.

In this study, optical signals were detected using a spectrometer consisting of a spectrograph (SpectraPro, Princeton Instruments, Acton, MA) equipped with a 300 lines/mm grating, connected to a front illuminated CCD camera (PI-MAX3 RB GEN II, Princeton Instruments, Acton) cooled to  $-25$  °C. The system was placed outside of the treatment room and light was collected using a 13 m long fiber bundle (Zlight, Latvia), comprised of seven 400  $\mu$ m diameter silica fibers in a hexagonal tip geometry, see Fig. 1. For every experiment, the fiber tip was placed in the center of the radiation beam at the phantom surface. An analog trigger out voltage was obtained from the linear accelerator control unit, and fed into the external trigger port of the CCD camera using a BNC cable. In an iterative manner, the delay between the falling edge of the trigger signal and rising edge of the linear accelerator beam on pulse was found to be 3  $\mu$ s. The trigger delay, gate width and frequency were used in conjunction with the LIGHTFIELD software package (Princeton Instruments, Acton, MA) for accurate gating and signal acquisition from the spectrometer-CCD coupled system, see Fig. 2.

Spectra were first acquired in a scattering phantom composed of phosphate buffered solution and 1% v/v Intralipid (Sigma Aldrich, Saint Louis, MO), see Fig. 3. For all experiments, a 4 $\times$ 4 cm 18 MeV  $\beta^-$  radiation beam at a dose rate of 4 Gy/min was used to maximize Cerenkov emission. Each spectrum was acquired at 100/100 $\times$  gain by averaging 1000 consecutive frames for a total acquisition time of approximately 6 seconds, corresponding to an acceptable treatment dose of  $\sim 40$  cGy. The gated signal spectrum was triggered externally by the linear accelerator with the beam and ambient lights on. Similarly, the ambient lights spectrum was triggered internally with the beam off and gating parameters identical to that of the gated signal. Isolation of the Cerenkov emission signal was obtained by calculating the difference between the two. All spectra were subject to background subtraction to account for characteristic system noise buildup at the high 100/100 $\times$  gain. The results, shown in Fig. 3a demonstrate that gated acquisition is successful in reducing the ambient lights signal to a low intensity DC signal similar to noise. For illustrative purposes, an auto-exposure white light image of the scattering phantom with ambient lighting levels used in all experiments was overlaid with a 30 second exposure image of the induced Cerenkov emission in the absence of ambient lights (Fig. 3b). Both images were captured using a CMOS camera (Rebel T3i, Canon, Tokyo, Japan) with a standard kit lens and the latter processed with a 20 $\times$ 20 pixel median filter in MATLAB 7.5.0 (The MathWorks Inc., Natick, MA).

To further explore the implications of this system for CES applications, tissue mimicking phantoms were mixed with phosphate buffered solution, 1% v/v Intralipid and 1% v/v porcine blood, see Fig. 4. Phantoms were deoxygenated using a glucose oxidase-catalase reaction (Thermo Fisher Scientific, Waltham, MA) and reference oxygenation saturation

measurements were performed using an ischemia monitoring system (Spectros T-Stat, Spectros, Portola Valley, CA)<sup>9</sup>. The absorption signatures due to hemoglobin are apparent in the acquired spectrum relative to the absence of an absorber and the isobestic points of oxy/deoxy hemoglobin easily visible in the 550–600 nm spectral region. Using a diffusion theory based fitting algorithm, these changes have been made quantitative in recovery of factors such as hemoglobin concentration and oxygen saturation which could have clinical significance in monitoring disease progression and treatment efficacy<sup>7</sup>.

The benefit of such a system can be realized when considering the importance of tumor oxygenation in the outcome of EBRT, as studies have shown hypoxic tumors to be less responsive to treatment due to inadequate damage to tumor DNA<sup>10,11</sup>. Additional clinical studies have also correlated tissue oxygen pressure (pO<sub>2</sub>) to EBRT effect in head and neck cancers and suggested that pO<sub>2</sub> increases during fractionated treatment plans<sup>12,13</sup>. Therefore there is great potential value in a non-invasive technique, such as CES for monitoring tumor oxygen saturation during EBRT. One previous issue with this modality was the inability to acquire signal in the presence of ambient room lighting. Due to the irradiance differences between commercial lighting and Cerenkov emission, previous studies in CW-CES acquisition were not feasible due to ambient light contamination. This inability to make measurements in a conventional radiation treatment environment raised concern for patient and physician compliance. However, the gated spectrometer-CCD system presented in this study offers a solution to this problem through a ~1000× reduction in ambient light contribution to the CES signal. While the experiments performed here involved relatively dim incandescent lights, future studies will work towards compatibility with fluorescent lighting, and creation of pick up fibers which have shaded regions to further suppress room light even in very bright light conditions. Despite their higher irradiance when compared to incandescent lights, fluorescent lights are inherently modulated at 60 Hz positive to negative voltage, emitting light at a frequency of 120 Hz. By incorporating the periodicity of the fluorescent lights into the gating timeline of the linear accelerator coupled spectrometer-CCD system, a situation could ideally be achieved with both components completely out of phase, thereby eliminating all fluorescent lighting contributions to the CES signal.

## Acknowledgments

This work was financially supported by NIH grants R01 CA120368 and R01 CA109558.

## References

1. Cerenkov PA. *Phys. Rev.* 1937; 52:378–379.
2. Robertson R, Germanos MS, Li C, Mitchell GS, Cherry SR, Silva MD. *Phys. Med. Biol.* 2009; 54:N355–N365. [PubMed: 19636082]
3. Spinelli AE, D'Ambrosio D, Calderan L, Marengo M, Sbarbati A, Boschi F. *Phys. Med. Biol.* 2010; 55:483–495. [PubMed: 20023328]
4. Liu H, Ren G, Miao Z, Zhang X, Tang X, Han P, Gambhir SS, Cheng Z. *PLoS ONE.* 2010; 5:e9470. [PubMed: 20208993]
5. Ruggiero A, Holland JP, Lewis JS, Grimm JJ. *Nucl. Med.* 2010; 51:1123–1130.
6. Li C, Mitchell GS, Cherry SR. *Opt. Lett.* 2010; 35(7):1109–1111. [PubMed: 20364233]
7. Axelsson J, Davis SC, Gladstone DJ, Pogue BW. *Med. Phys.* 2011; 38(7):4127. [PubMed: 21859013]
8. Axelsson J, Glaser AK, Gladstone DJ, Pogue BW. 2011 Submitted.
9. Brody, LA.; Strupinsky, ER.; Kline, LR. *Active packaging for food applications.* Vol. Chap. 3. CRC Press; 2001.
10. Vaupel, P.; Mayer, A.; Höckel, M. *Recombinant Human Erythropoietin (rhEPO) in Clinical Oncology.* Mohammad Resa Nowrousian. , editor. Springer Vienna: 2008. p. 265-282.

11. Evans SM, Koch CJ. *Cancer Lett.* 2003; 195:1–16. [PubMed: 12767506]
12. Nordmark M, Bentzen SM, Rudat V, Brizel D, Lartigau E, Stadler P, Becker A, Adam M, Molls M, Dunst J, Terris DJ, Overgaard J. *Radiother. Oncol.* 2005; 77:18–24. [PubMed: 16098619]
13. Cooper RA, West CM, Logue JP, Davidson SE, Miller A, Roberts S, Statford IJ, Honess DJ, Hunter RD. *Int. J. Radiat. Oncol. Biol. Phys.* 1999; 45:119–126. [PubMed: 10477015]

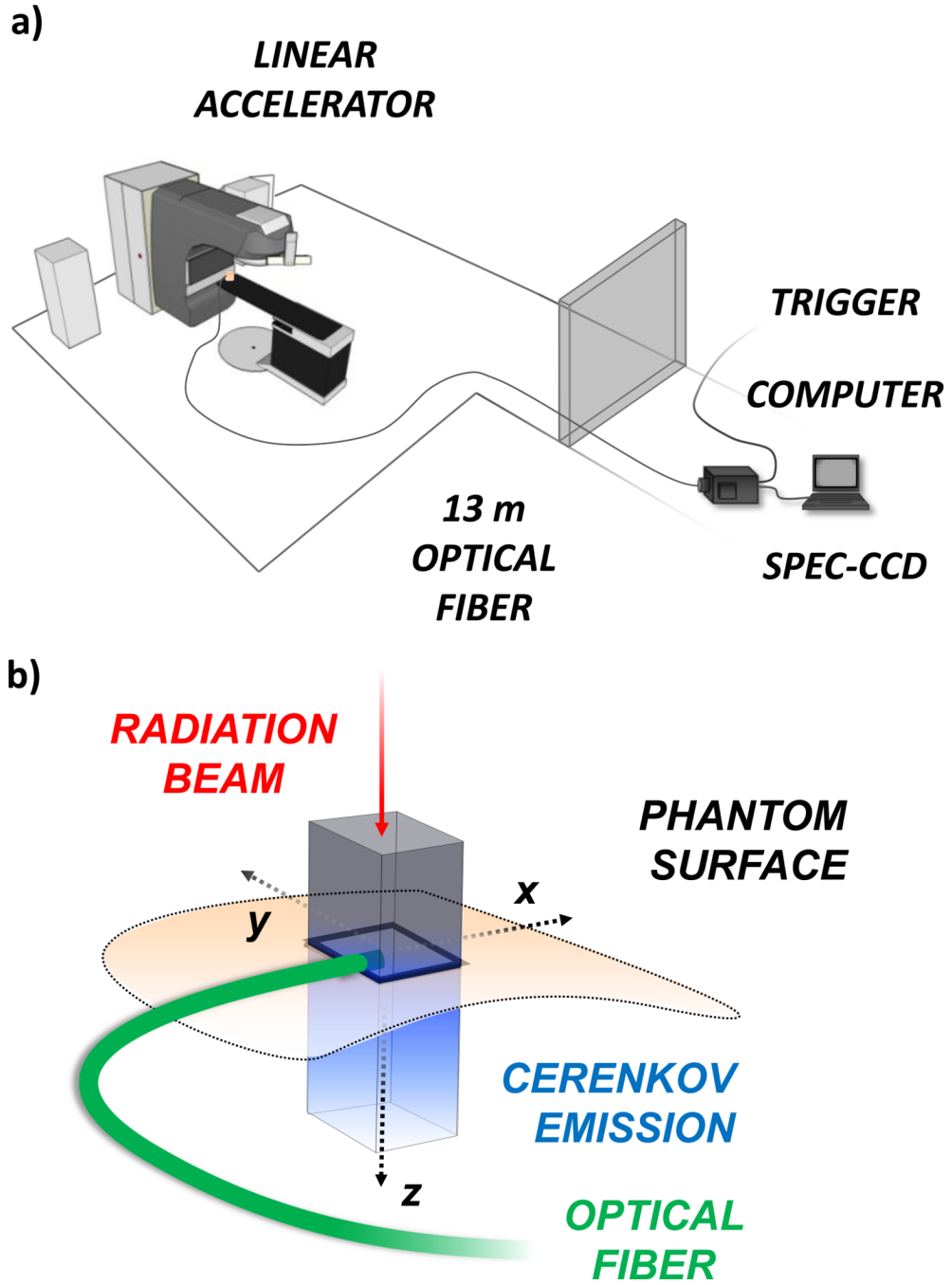


**Fig. 1.** (color online) In (a) the experimental setup is shown with the computer controlled spectrometer-CCD system located outside of the treatment room, and light collected through a 13 m long optical fiber. The trigger was obtained from the LINAC external control unit. In (b) a schematic of Cerenkov emission in a phantom is illustrated. The radiation beam travels downward with a rectangular cross-section producing a column of Cerenkov emission below the surface. The optical fiber is placed on the phantom surface with the tip in the center of the radiation beam.

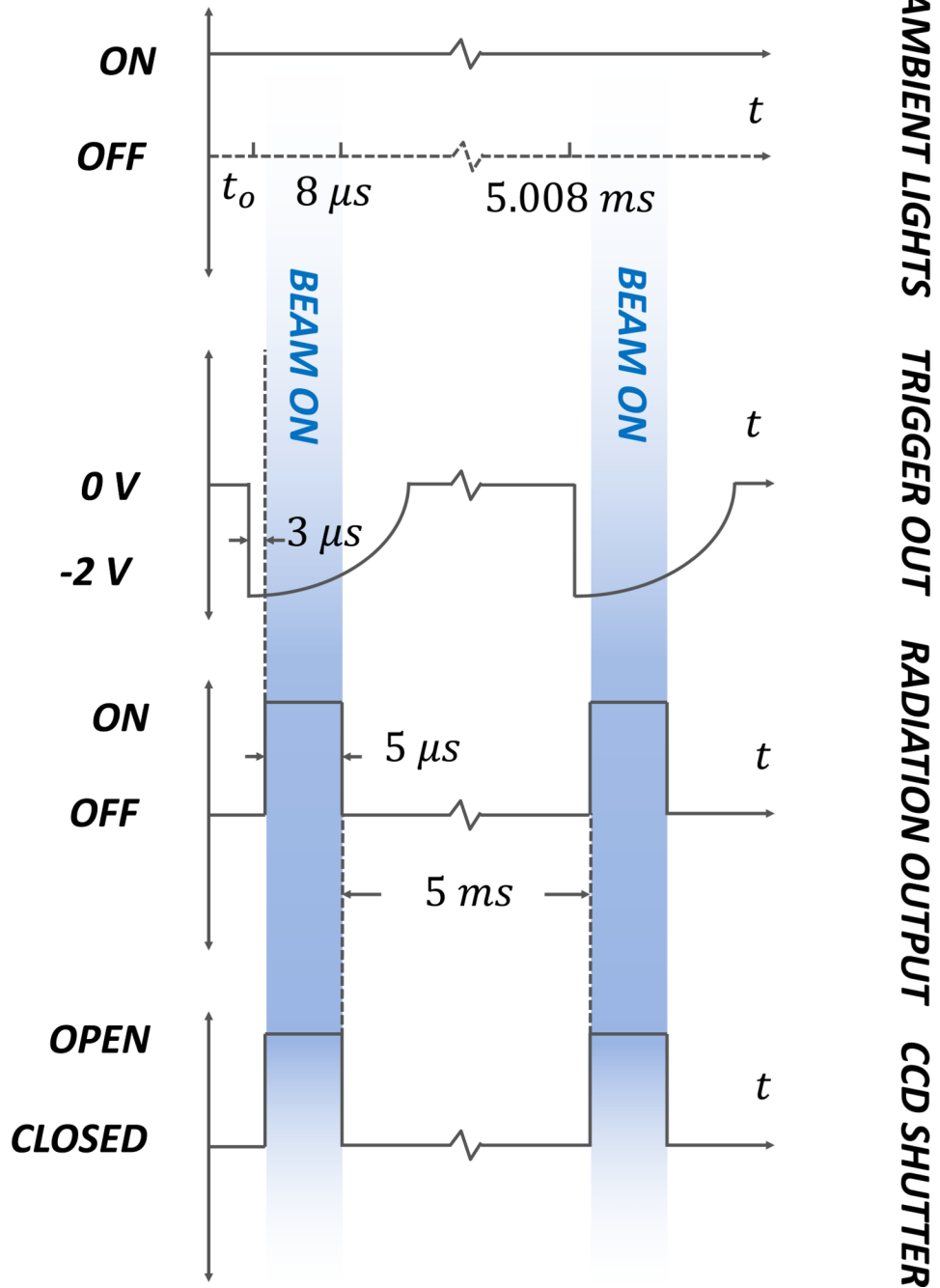


**Fig. 2.** (color online) The timeline of events for the ambient lights, output trigger, radiation beam output, and CCD shutter are shown. The periods of beam on and subsequent Cerenkov emission are shown in shaded blue.

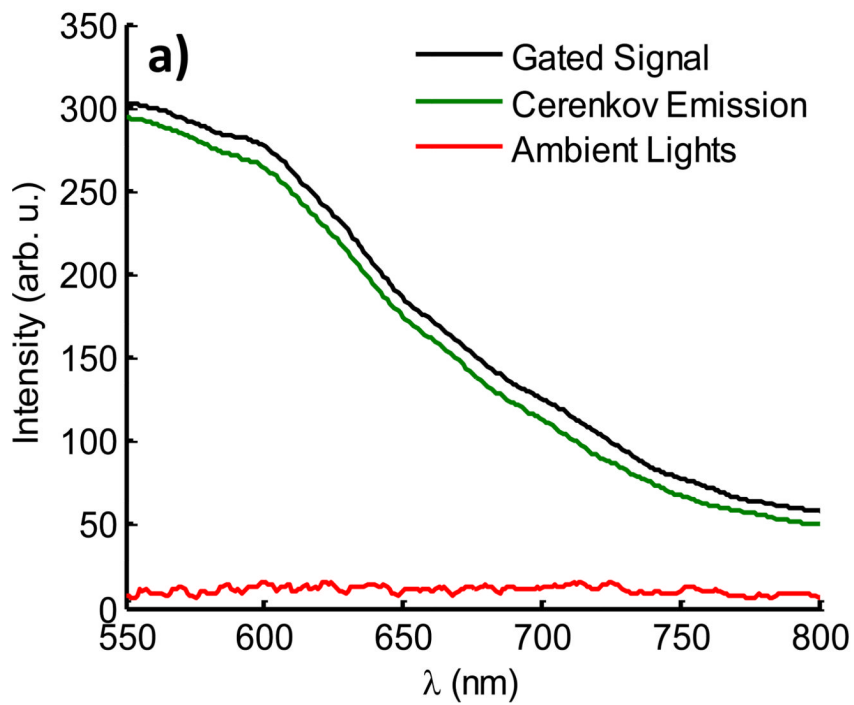


**Fig. 3.** (color online) The gated detection of Cerenkov emission with room lights on is shown with spectra acquired from a scattering phantom, left. The Cerenkov emission is obtained by calculating the difference between the gated signal and ambient lighting signal. A photograph of the room with a corresponding image of Cerenkov emission from the scattering phantom are overlaid to illustrate the amount of ambient lighting present for all experiments.

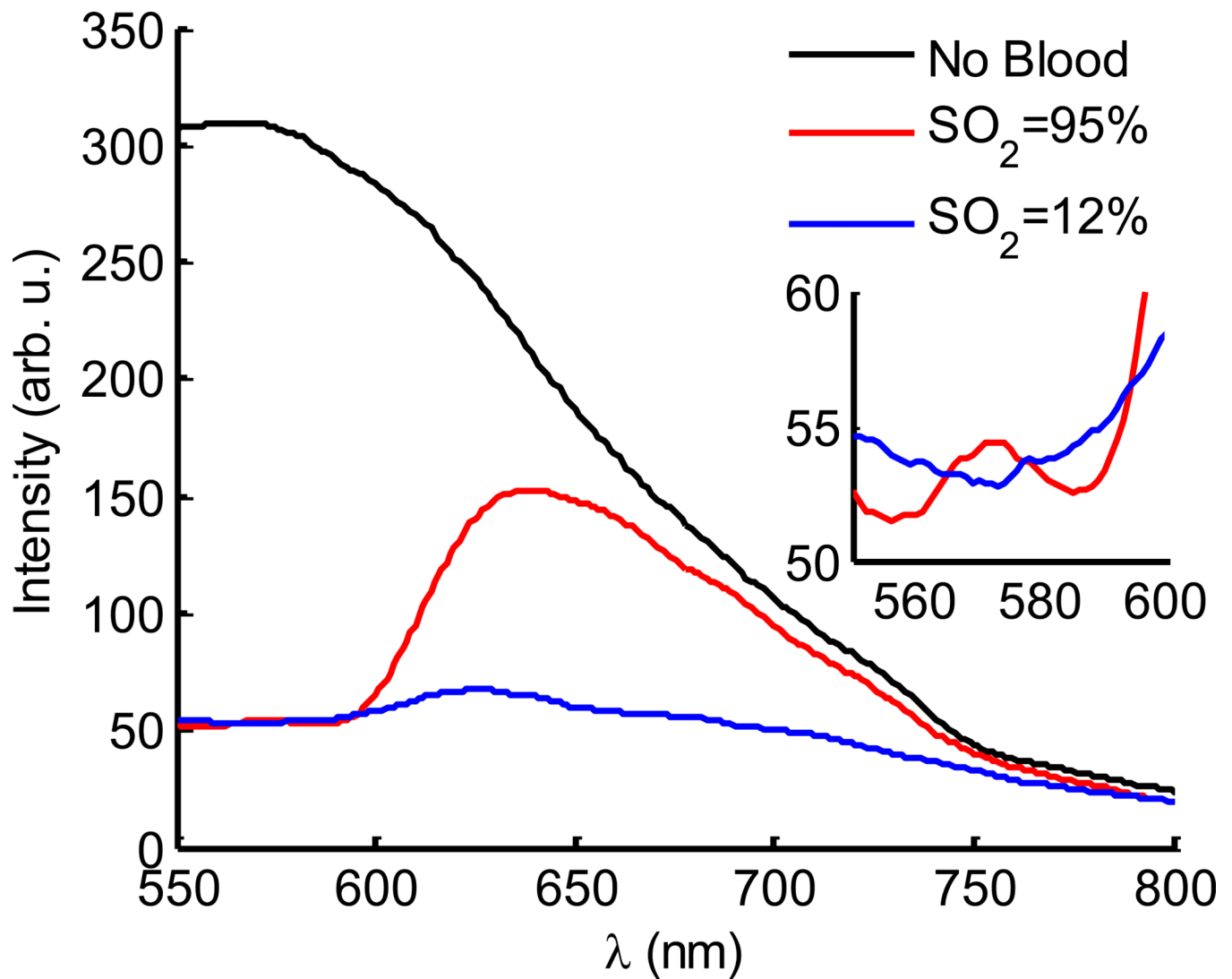


**Fig. 4.** (color online) The gated detection of Cerenkov emission in a tissue simulating phantom is shown in with spectra of a phantom having no blood (black line), as well as oxygenated and deoxygenated blood are shown (red and blue lines). The inset highlights the isobestic region in the 550–600 nm spectral region.